

# Blue upconversion luminescence in $\text{Tm}^{3+}/\text{Yb}^{3+}$ co-doped new oxyfluoride tellurite glass

Shiqing Xu (徐时清)<sup>1,2,3</sup>, Hongping Ma (马红萍)<sup>4</sup>, Dawei Fang (方达伟)<sup>1</sup>,  
Zaixuan Zhang (张在宣)<sup>1</sup>, Lili Hu (胡丽丽)<sup>2</sup>, and Zhonghong Jiang (姜中宏)<sup>2</sup>

<sup>1</sup>Institute of Optoelectronic Materials and Devices,

College of Information Engineering, China Jiliang University, Hangzhou 310018

<sup>2</sup>Shanghai Institute of Optics and Fine Mechanics, Chinese Academy of Sciences, Shanghai 201800

<sup>3</sup>Graduate School of Chinese Academy of Sciences, Beijing 100039

<sup>4</sup>Department of Mechanical and Electrical, Zhejiang University of Science and Technology, Hangzhou 310012

Received December 28, 2004

The thermal stability, Raman spectrum and upconversion properties of  $\text{Tm}^{3+}/\text{Yb}^{3+}$  co-doped new oxyfluoride tellurite glass are investigated. The results show that  $\text{Tm}^{3+}/\text{Yb}^{3+}$  co-doped oxyfluoride tellurite glass possesses good thermal stability, lower phonon energy, and intense upconversion blue luminescence. Under 980-nm laser diode (LD) excitation, the intense blue (475 nm) emission and weak red (649 nm) emission corresponding to the  $^1G_4 \rightarrow ^3H_6$  and  $^1G_4 \rightarrow ^3F_4$  transitions of  $\text{Tm}^{3+}$  ions respectively, were simultaneously observed at room temperature. The possible upconversion mechanisms are evaluated. The intense blue upconversion luminescence of  $\text{Tm}^{3+}/\text{Yb}^{3+}$  co-doped oxyfluoride tellurite glass can be used as potential host material for the development of blue upconversion optical devices.

OCIS codes: 160.4670, 160.4760, 160.2750, 160.2540.

Solid-state blue and green light sources are desirable for high-density optical storage, color displays, optoelectronics, and medical diagnostics<sup>[1-4]</sup>.  $\text{Tm}^{3+}$  is the most studied in rare-earth ions for blue laser operation based upon upconversion<sup>[5,6]</sup>. One approach to improving the luminescence efficiency of  $\text{Tm}^{3+}$  is to co-dope it with other rare-earth ions<sup>[7]</sup>. The choice of host materials is a very important factor to obtain high efficient upconversion emission. In this case, the main goal of the choice of host materials is to increase the luminescence (radiative emission) efficiency by reducing non-radiative loss due to the multiphonon relaxation. It is possible to use glass hosts with low-phonon energies such as fluoride glasses, but these glasses present poor mechanical, thermal, and chemical stability<sup>[8]</sup>. However, for various hosts, the conventional oxide glasses such as phosphate, silicate, and borate glasses are difficult to produce strong upconversion emission owing to their high phonon energies<sup>[9]</sup>. Therefore, there must be a compromise between low phonon energy and good environmental stability for device operation purposes.

As is known, glasses based on mixed oxide-fluoride systems combine the good optical properties of halide glasses (a broad range of optical transmittance and low optical losses) with the better chemical and thermal stability of oxide glasses<sup>[10]</sup>. In this letter, we report on the experimental investigation of thermal stability, Raman spectrum and upconversion luminescence of  $\text{Tm}^{3+}/\text{Yb}^{3+}$  co-doped new oxyfluoride tellurite glass. The results demonstrate that they can act as suitable materials for practical upconversion applications.

The glass sample was prepared from  $\text{TeO}_2$  (99.99%),  $\text{PbF}_2$  (99.9%),  $\text{Yb}_2\text{O}_3$  (99.99%), and  $\text{Tm}_2\text{O}_3$  (99.99%) according to the following compositions in mol%:  $60\text{TeO}_2\text{-}40\text{PbF}_2\text{-}3\text{Yb}_2\text{O}_3\text{-}0.1\text{Tm}_2\text{O}_3$  (TPF). A glass sam-

ple with compositions in mol%:  $70\text{TeO}_2\text{-}25\text{ZnO}\text{-}2\text{Na}_2\text{O}\text{-}0.1\text{Tm}_2\text{O}_3\text{-}3\text{Yb}_2\text{O}_3$  (TZN) was prepared for comparison of thermal stability and upconversion luminescence intensity with TPF glass. About batch of 50 g of starting materials was fully mixed and then melted in the covered platinum crucibles at 700–800 °C in an electronic furnace with a  $\text{N}_2$  atmosphere. When the melting was completed, the glass liquids were cast into stainless steel plates. The obtained glass sample was cooled to room temperature at a rate of 10 °C/h, and then was cut and polished carefully in order to meet the requirements for optical measurements. The glass transition temperature ( $T_g$ ) and crystallization onset temperature ( $T_x$ ) were determined by differential scanning calorimetry (DSC) at a heating rate of 10 °C/min, using aluminum oxide ceramic pan. The upconversion luminescence spectrum was obtained with a TRIAX550 spectrofluorimeter upon excitation of 980-nm laser diode (LD) with a maximum power of 2 W. The Raman spectrum was recorded on a Fourier transform (FT) Raman spectrophotometer (Nicolet MODULE) within the range of 100–1200  $\text{cm}^{-1}$ . Nd:YAG operating at 1064 nm is used as the excitation source. All the measurements were taken at room temperature.

The DSC curve of  $\text{Tm}^{3+}/\text{Yb}^{3+}$  co-doped TPF glass is illustrated in Fig. 1. The quantity,  $\Delta T = T_x - T_g$ , has been frequently used as a rough estimate of the glass stability. To achieve a large working range of temperature during our sample fiber drawing, it is desirable for a glass host to have  $\Delta T$  as large as possible<sup>[11]</sup>. From Fig. 1, it can be seen that the  $\Delta T$  value of  $\text{Tm}^{3+}/\text{Yb}^{3+}$  co-doped TPF glass is 123 °C, which is larger than that of TZN glass (118 °C)<sup>[12]</sup>, indicating TPF glass with good thermal stability.

Figure 2 shows the Raman spectrum of the undoped

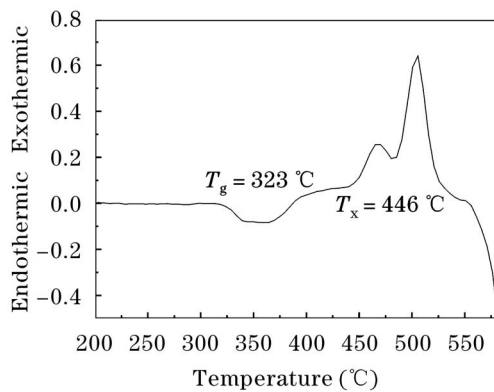


Fig. 1. The differential scanning calorimetry curve of  $\text{Tm}^{3+}/\text{Yb}^{3+}$  co-doped TPF glass.

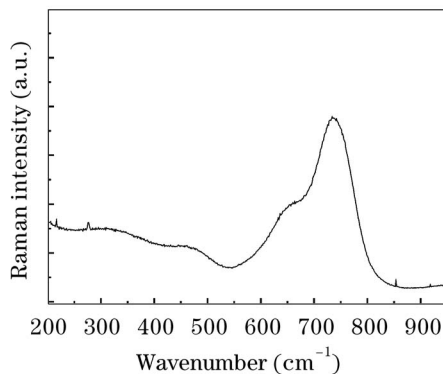


Fig. 2. The Raman spectrum of the undoped TPF glass at room temperature.

TPF glass at room temperature. The Raman spectrum indicates that the phonon energy of TPF glass is at  $734 \text{ cm}^{-1}$ , which is lower than those of tellurite, germanate, silicate, phosphate, and borate glasses<sup>[13]</sup>. The broad modes around  $445 \text{ cm}^{-1}$  assigned to bending vibrations of Te-O-Te linkages,  $654 \text{ cm}^{-1}$  due to the stretching vibrations of  $\text{TeO}_4$  bipyramids,  $734 \text{ cm}^{-1}$  due to the stretching vibrations of  $\text{TeO}_3$  and/or  $\text{TeO}_{3+1}$  trigonal pyramids<sup>[14,15]</sup>.  $\text{PbF}_2$  added in the glass lowers the maximum phonon energy of tellurite glasses, and thus it reduces the nonradiative loss due to the multiphonon relaxation, and can enhance radiative transition and upconversion luminescence intensity of  $\text{Tm}^{3+}$  in oxyfluoride tellurite glass.

The room temperature upconversion luminescence spectra in the range of 400–700 nm for  $\text{Tm}^{3+}/\text{Yb}^{3+}$  co-doped TPF and TZN glasses under 980-nm LD excitation are shown in Fig. 3. It can be observed that the signal light emanating from sample presented two distinct emission bands centered around 475 and 649 nm, corresponding to the  ${}^1G_4 \rightarrow {}^3H_6$  and  ${}^1G_4 \rightarrow {}^3F_4$  transitions of  $\text{Tm}^{3+}$  ions, respectively. The blue emission in the region from 450 to 510 nm for  $\text{Tm}^{3+}/\text{Yb}^{3+}$  co-doped TPF glass is dominant, accounting for 88% of the total emitted light in the spectral region from 400 to 700 nm. It is important to mention at this point that the blue emission around 475 nm was intense enough to be seen by naked eyes at excitation power as low as 50 mW. The upconversion luminescence intensity of  $\text{Tm}^{3+}/\text{Yb}^{3+}$  co-doped TPF glass is much bigger than that of TZN glass.

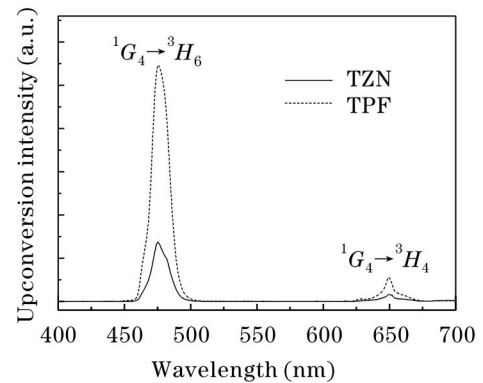


Fig. 3. Upconversion emission spectra of  $\text{Tm}^{3+}/\text{Yb}^{3+}$  co-doped TPF and TZN glasses under 980-nm excitation at room temperature.

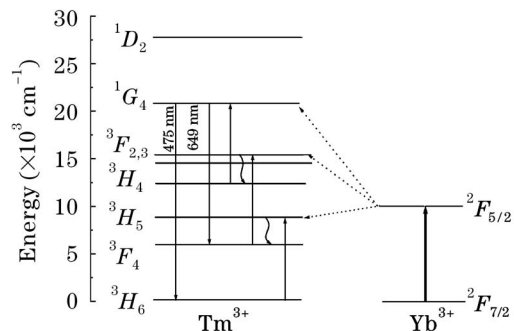


Fig. 4. Simplified energy level diagram of  $\text{Tm}^{3+}$  and  $\text{Yb}^{3+}$  and possible transition pathways yielded under 980 nm excitation. The dashed arrows represent the energy transfer processes. The wave lines stand for multiphonon nonradiative relaxation processes.

According to the energy matching conditions, the possible upconversion mechanisms for the emission bands are discussed based on the energy level of  $\text{Tm}^{3+}$  and  $\text{Yb}^{3+}$  presented in Fig. 4<sup>[16,17]</sup>. The excitation process for the  ${}^1G_4 \rightarrow {}^3H_6$  and  ${}^1G_4 \rightarrow {}^3F_4$  transitions can be explained as follows. In the first step, a 980-nm photon is absorbed by an  $\text{Yb}^{3+}$  which provokes the  ${}^2F_{7/2} \rightarrow {}^2F_{5/2}$  transition. The second step involves the excitation of a  $\text{Tm}^{3+}$  in the  ${}^3H_5$ , by means of the energy transfer mechanism of excited  $\text{Yb}^{3+}$  to  $\text{Tm}^{3+}$ .  $\text{Tm}^{3+}$  in the  ${}^3H_5$  excited state relaxes nonradiatively to the metastate level  ${}^3F_4$ . As the third step, either the same  $\text{Yb}^{3+}$  which absorbs a second 980 nm photon or another nearby  $\text{Yb}^{3+}$  being still in the  ${}^2F_{5/2}$  state, transfers its energy to the same  $\text{Tm}^{3+}$ , and the mechanism in which the  $\text{Tm}^{3+}$  in the excited state  ${}^3F_4$  absorbs a 980-nm photon is also possible. The  $\text{Tm}^{3+}$  reaches the  ${}^3F_{2,3}$  level and the  ${}^3F_{2,3}$  state also relaxes by a multiphonon assisted process to the  ${}^3H_4$  level. Finally, the population of  ${}^1G_4$  is based on the processes as follows: energy transfer from  $\text{Yb}^{3+}$ :  ${}^2F_{5/2}(\text{Yb}^{3+}) + {}^3H_4(\text{Tm}^{3+}) \rightarrow {}^2F_{7/2}(\text{Yb}^{3+}) + {}^1G_4(\text{Tm}^{3+})$ , and excited state absorption:  ${}^3H_4(\text{Tm}^{3+}) + \text{photon} \rightarrow {}^1G_4(\text{Tm}^{3+})$ . From the  ${}^1G_4$  level, the  $\text{Tm}^{3+}$  ions decay radiatively to the  ${}^3H_6$  ground state generating the intense blue emission around 475 nm. The major contribution to the red (649 nm) emission is attributed to the  ${}^1G_4 \rightarrow {}^3F_4$  transition, while the transition probability involved in the above processes is small, the red emission observed is weak. From

the above results it can be concluded that a three-phonon upconversion process is responsible for blue (475 nm) and red (649 nm) emissions.

In conclusion, the thermal stability, Raman spectrum, and upconversion properties of  $\text{Tm}^{3+}/\text{Yb}^{3+}$  co-doped new oxyfluoride tellurite glass under 980-nm LD excitation were investigated. The thermal stability of  $\text{Tm}^{3+}/\text{Yb}^{3+}$  co-doped glass is better than that of TZN glass. The maximum phonon energy of oxyfluoride tellurite glass is lower than those of tellurite, germanate, silicate, phosphate, and borate glasses. The upconversion luminescence intensity of  $\text{Tm}^{3+}/\text{Yb}^{3+}$  co-doped TPF glass is much bigger than that of TZN glass. The blue emission in the region from 450 to 510 nm for  $\text{Tm}^{3+}/\text{Yb}^{3+}$  co-doped TPF glass is dominant, accounting for 88% of the total emitted light in the spectral region from 400 to 700 nm. A three-photon upconversion process is assigned to the blue (476 nm) and red (649 nm) emissions. The obtained results in this study might provide useful information for development of blue upconversion lasers.

This work was supported by the National Nature Science Foundation of China under Grant No. 60207006. S. Xu's e-mail address is shiqingxu75@hotmail.com.

## References

1. S. O. Man, E. Y. B. Pun, and P. S. Chung, *Appl. Phys. Lett.* **77**, 483 (2000).
2. L. H. Huang, X. R. Liu, W. Xu, B. J. Chen, and J. L. Lin, *J. Appl. Phys.* **90**, 5550 (2001).
3. S. Q. Xu, Z. M. Yang, J. J. Zhang, G. N. Wang, S. X. Dai, L. L. Hu, and Z. H. Jiang, *Chem. Phys. Lett.* **385**, 263 (2004).
4. S. Q. Xu, Z. M. Yang, S. X. Dai, G. N. Wang, L. L. Hu, and Z. H. Jiang, *Mater. Lett.* **58**, 1026 (2004).
5. M. Tsuda, K. Soga, H. Inoue, S. Inoue, and A. Makishima, *J. Appl. Phys.* **85**, 29 (1999).
6. S. Q. Xu, J. J. Zhang, G. N. Wang, S. X. Dai, L. L. Hu, and Z. H. Jiang, *Chin. Phys. Lett.* **21**, 927 (2004).
7. J. Qiu and Y. Kawamoto, *J. Fluorine Chem.* **110**, 175 (2001).
8. S. Xu, Z. Yang, G. Wang, S. Dai, L. Hu, and Z. Jiang, *Chin. Opt. Lett.* **1**, 544 (2003).
9. S. Q. Xu, Z. M. Yang, G. N. Wang, J. J. Zhang, S. X. Dai, L. L. Hu, and Z. H. Jiang, *Spectrochimica Acta Part A* **60**, 3025 (2004).
10. S. Q. Xu, G. N. Wang, J. J. Zhang, S. X. Dai, L. L. Hu, and Z. H. Jiang, *J. Non-Cryst. Solids* **336**, 230 (2004).
11. S. Xu, S. Dai, J. Zhang, L. Hu, and Z. Jiang, *Chin. Opt. Lett.* **2**, 106 (2004).
12. J. S. Wang, E. M. Vogel, and E. Snitzer, *Opt. Mater.* **3**, 187 (1994).
13. Z. Pan, S. H. Morgan, A. Loper, V. King, B. H. Long, and W. E. Collins, *J. Appl. Phys.* **77**, 4688 (1995).
14. A. Jha, S. Shen, and M. Naftaly, *Phys. Rev. B* **63**, 6215 (2000).
15. S. Q. Xu, H. T. Sun, S. X. Dai, J. J. Zhang, and Z. H. Jiang, *Solid State Commun.* **133**, 89 (2005).
16. F. C. Guinhos, P. C. Nóbrega, and P. A. Santa-Cruz, *J. Alloys and Compounds* **323—324**, 358 (2001).
17. M. V. D. Vermelho, M.T. de Araujo, E. A. Gouveia, A. S. Gouveia-Neto, and J. S. Aitchison, *Opt. Mater.* **17**, 419 (2001).